

## First-Principles Calculations of Vibrational Lifetimes and Decay Channels: Hydrogen-Related Modes in Si

D. West and S. K. Estreicher\*

*Physics Department, Texas Tech University, Lubbock, Texas 79409-1051, USA*

(Received 5 January 2006; published 22 March 2006)

The vibrational lifetimes and decay channels of local vibrational modes are calculated from first principles at various temperatures. Our method can be used to predict the temperature dependence of the lifetime of any normal mode in any crystal. We focus here on the stretch modes of  $H_2^*$ ,  $H_{BC}^+$ , and  $VH \cdot HV$  in Si. The frequencies are almost identical, but the lifetimes vary from 4 to 295 ps. The calculations correctly predict the lifetimes for  $T > 50$  K and illustrate the critical importance of pseudolocal modes in the decay processes of high-frequency local vibrational modes.

DOI: [10.1103/PhysRevLett.96.115504](https://doi.org/10.1103/PhysRevLett.96.115504)

PACS numbers: 63.20.Mt, 61.72.Bb

The relaxation dynamics of impurity-related local vibrational modes (LVMs) in crystal are unpredictable. Indeed, the lifetimes of nearly identical high-frequency modes are observed to differ by up to 2 orders of magnitude. Since these decays should not involve fewer than five crystal phonons, the short lifetimes sometimes observed imply that some LVMs couple to the phonon bath much more efficiently than others. Although the temperature dependence of the lifetimes can be fitted to a general formula, the mechanisms involved in the fastest decay processes are not at all understood.

The passivation by H or D of Si dangling bonds at the Si/SiO<sub>x</sub> interface ( $P_b$  center) [1,2] illustrates the importance of vibrational lifetimes. The devices treated with D have transconductance lifetimes 10–50 times longer than those treated with H [3]. Inelastic scattering with hot electrons excites the LVMs of the Si-H or Si-D bond. The dissociation rate depends critically on the vibrational lifetimes [4,5].

The lifetimes of several H-related stretch LVMs in Si have been measured by transient bleaching spectroscopy [6,7]. The low temperatures lifetimes of the 2062 cm<sup>-1</sup> mode of  $H_2^* = Si-H_{BC} \cdots Si-H_{AB}$  [8] (BC and AB stand for bond-centered and antibonding, respectively), the 1998 cm<sup>-1</sup> mode of  $H_{BC}^+$  [6,9], and the 2072 cm<sup>-1</sup> mode of the divacancy dihydrogen complex [8,10]  $VH \cdot HV$  are 4, 8, and 295 ps (that is,  $\sim 250$ , 480, and 18 000 oscillations), respectively. Since the optical phonon of Si is  $\sim 530$  cm<sup>-1</sup>, the decays should involve at least four phonons and all these LVMs should have long lifetimes.

All vibrational lifetimes exhibit a strong temperature dependence and fall off at higher temperatures. A general expression for the temperature dependence of the lifetimes [11,12] has been used to fit the experimental data to sets of accepting modes [6,8]. In the case of  $H_{BC}^+$ , the fit yields three acoustic ( $\sim 150$  cm<sup>-1</sup>) and three optic ( $\sim 520$  cm<sup>-1</sup>) phonons. Although this fit is not unique, a fit using just four accepting modes at 500 cm<sup>-1</sup> fails to fit the data. A good fit is also obtained for  $VH \cdot HV$  with three acoustic

( $\sim 343$  cm<sup>-1</sup>) and two optic ( $\sim 520$  cm<sup>-1</sup>) phonons. Thus, the theoretical model fails to explain why an 8 ps lifetime should involve six phonons while a 295 ps one only five.

The measurements of the lifetimes of H-related wag modes [13] yield a more straightforward explanation. These lifetimes vary exponentially with the frequency separation between the LVM and the receiving modes (“frequency-gap law”). The farther away a LVM is from the host crystal’s phonon bands, the longer the lifetime as the decay involves an increasing number of phonons.

Bulk vibrational lifetimes in amorphous Si have been estimated using the Stillinger-Weber potential by calculating decay rates [14] and by monitoring the exponential decay of initial velocity amplitudes in molecular-dynamics (MD) simulations at low temperatures [15]. Tight-binding MD simulations have also been used [5] to calculate the lifetime of the degenerate wag modes of Si-H and Si-D bonds on an Si(111) surface, by displacing the H or D atom along the eigenmode and monitoring the decay of the oscillation in a network at  $T = 0$  K.

In this work, we develop a first-principles scheme to calculate vibrational lifetimes and decay channels at various temperatures. The calculations predict the correct lifetimes for  $H_2^*$ ,  $H_{BC}^+$ , and  $VH \cdot HV$  and provide insights into the decay mechanism(s). In the case of  $H_2^*$ , the receiving modes are unambiguously identified.

We use the SIESTA [16,17] code in 64 host-atoms supercells. Norm-conserving pseudopotentials in the Kleinman-Bylander form [18] describe the core regions. The valence regions are treated within first-principles local density-functional theory with the exchange-correlation potential of Ceperley-Alder [19] parametrized by Perdew-Zunger [20]. The (double-zeta) basis sets for the valence states are linear combinations of numerical atomic orbitals [21]. The charge density is projected on a real-space grid with equivalent cutoffs of 80 Ry to calculate the exchange-correlation and Hartree potentials. The dynamical matrices are obtained from linear-response theory [22–24]. Their eigenvalues are the normal-mode frequencies  $\omega_s$ , and the

(orthonormal) eigenvectors  $e_{\alpha i}^s$  give the relative displacements of the nuclei ( $\alpha$  numbers the nuclei,  $i = x, y, z$ ).

Figure 1 shows the square of the eigenvectors associated with the H atom(s) and the two Si atoms it (they) are bound vs  $\omega$ . For  $\text{H}_2^*$  (top), the stretch modes are at  $2126 \text{ cm}^{-1}$  for Si-H<sub>BC</sub> (measured [8]  $2062 \text{ cm}^{-1}$ ) and  $1860 \text{ cm}^{-1}$  for Si-H<sub>AB</sub> (measured [25]  $1844 \text{ cm}^{-1}$ ). The doublets at  $853$  and  $457 \text{ cm}^{-1}$  are the wag modes of H<sub>AB</sub> and H<sub>BC</sub>, respectively. The asymmetric stretch of H<sub>BC</sub><sup>+</sup> (middle) is at  $2014 \text{ cm}^{-1}$  (measured [6]  $1998 \text{ cm}^{-1}$ ), and the wag modes are at  $261 \text{ cm}^{-1}$ . The modes at  $209$  and  $410 \text{ cm}^{-1}$  involve the two Si neighbors of H: The two Si atoms move together or opposite each other along the trigonal axis, respectively. In VH·HV (bottom), the degenerate Si-H stretch modes are at  $2092 \text{ cm}^{-1}$  (measured [8]  $2072 \text{ cm}^{-1}$ ), and the four closely spaced modes near  $597 \text{ cm}^{-1}$  are the H wag modes.

The eigenvectors  $e_{\alpha i}^s$  are needed to transform the (harmonic) normal-mode coordinates  $q_s = A_s(T)\cos(\omega_s t + \varphi_s)$  into Cartesian nuclear displacements

$$u_{\alpha i} = \frac{1}{\sqrt{m_\alpha}} \sum_s q_s e_{\alpha i}^s.$$

In thermal equilibrium, the *average* kinetic energy of each mode is  $k_B T/2$ , that is,

$$\langle \frac{1}{2} \dot{q}_s^2 \rangle = \langle \frac{1}{2} \omega_s^2 A_s^2 \sin^2(\omega_s t + \varphi_s) \rangle = \frac{1}{4} \omega_s^2 \langle A_s^2 \rangle = \frac{1}{2} k_B T.$$

Thus, on the average,  $\langle A_s \rangle = \sqrt{2k_B T}/\omega_s$ . If  $A_s = \langle A_s \rangle$  for all  $s$ , the energy of each mode is exactly  $k_B T$ . Instead, we use a random distribution

$$\zeta_s = \int_0^{E_s} \frac{1}{k_B T} e^{-E/k_B T} dE,$$

with  $0 < \zeta_s < 1$ , and  $A_s = \sqrt{-2k_B T \ln(1 - \zeta_s)}/\omega_s$  leads to a distribution of normal-mode energies which averages out to  $k_B T$ .

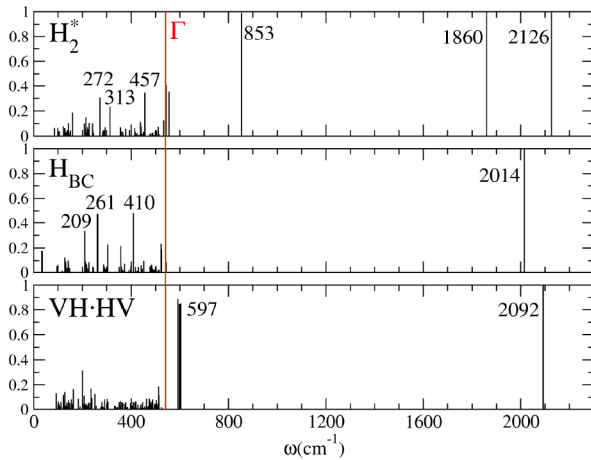


FIG. 1 (color online). Plots of  $\sum_{\alpha,i} (e_{\alpha i}^s)^2$  (where  $\alpha = \text{H}'\text{s}$  and the two Si atoms bound to them) vs frequency. The vertical line ( $\Gamma$ ) is the calculated optical mode of Si.

Therefore, in equilibrium at the temperature  $T$ , the (harmonic) Cartesian positions and velocities are

$$u_{\alpha i} = \sqrt{\frac{2k_B T}{m_\alpha}} \sum_s \frac{1}{\omega_s} \sqrt{-\ln(1 - \zeta_s)} \cos(\omega_s t + \varphi_s) e_{\alpha i}^s$$

and

$$\dot{u}_{\alpha i} = -\sqrt{\frac{2k_B T}{m_\alpha}} \sum_s \sqrt{-\ln(1 - \zeta_s)} \sin(\omega_s t + \varphi_s) e_{\alpha i}^s.$$

The random phases  $0 \leq \varphi_s < 2\pi$  ensure that each mode has a random amount of kinetic and potential energy. We use these initial ( $t = 0$ ) positions and velocities to prepare the supercell in equilibrium at the temperature  $T$ . Tests of these initial conditions in the range  $50 < T < 500 \text{ K}$  show that the temperature fluctuates around  $T$  with very small and almost perfectly constant amplitudes from step 1. No thermalization or thermostat are needed. This procedure is similar to that described in Ref. [26].

We excite the LVM under study by assigning it the kinetic energy  $3\hbar\omega/2$  (zero-point energy plus one phonon) in the supercell in thermal equilibrium at the temperature  $T$ . This excitation is achieved using the appropriate eigenvector of the dynamical matrix. The slight increase in the temperature it causes is small compared to the background temperature of the cell. Note that we always use the same initial excitation of the LVM and vary the equilibrium temperature of the cell, an approach that mimics the experimental procedure. The constant-temperature MD run is performed at the temperature  $T$  with a time step of  $0.3 \text{ fs}$ . At every time step, we transform the  $3N$  Cartesian coordinates of the  $N$  nuclei into linear combinations of the  $3N$  normal modes. The amplitudes allow us to calculate the energy of every normal mode as a function of (real) time, at the temperature  $T$ .

Figure 2 shows the energy of the four highest-frequency modes of  $\text{H}_2^*$  at  $T = 50 \text{ K}$ , with  $A$  denoting the Si-H<sub>BC</sub> stretch ( $2126 \text{ cm}^{-1}$ ),  $B$  denoting the Si-H<sub>AB</sub> stretch

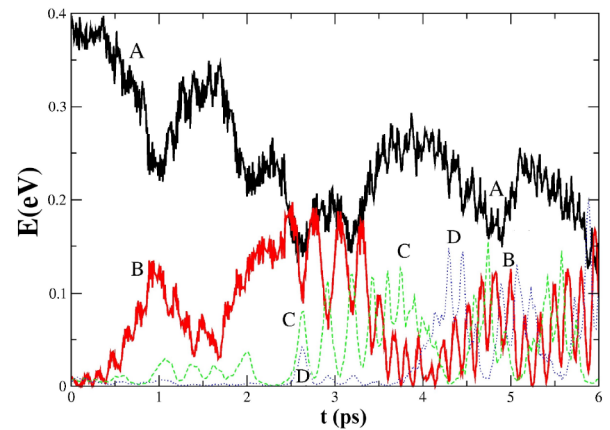


FIG. 2 (color online). Time evolution of the energies of the four highest-frequency modes of  $\text{H}_2^*$  at  $T = 50 \text{ K}$ .

(1860  $\text{cm}^{-1}$ ), and  $C$  and  $D$  denoting the degenerate wag modes of  $H_{AB}$  (853  $\text{cm}^{-1}$ ) and  $H_{BC}$  (457  $\text{cm}^{-1}$ ), respectively. During the first 2 ps,  $A$  decays into  $B$  plus the mode at 272  $\text{cm}^{-1}$  (Fig. 1), which involves the two Si atoms in  $H_2^*$  oscillating against each other, while the 2 H atoms remain essentially still. The wag modes  $C$  and  $D$  control the decay of the 1860  $\text{cm}^{-1}$  mode ( $B$ ). The energy is then transferred from  $C$  and  $D$  into bulk phonons.

Thus, the decay of the 2126  $\text{cm}^{-1}$  mode of  $H_2^*$  is not a six-phonon process as assumed [8] but a two-phonon process (1860 and 272  $\text{cm}^{-1}$ ), and the lifetime fits on the frequency-gap law [13]. Both phonons are localized on the  $H_2^*$  defect.

The case of  $H_{BC}^+$  is more complicated. There is no LVM other than the 2014  $\text{cm}^{-1}$  mode. Therefore, its decay cannot involve fewer than four phonons and its lifetime does not fit on the frequency-gap law. The modes associated with  $H_{BC}^+$  (Fig. 1) are the asymmetric stretch at 2014  $\text{cm}^{-1}$ , the two wag modes at 261  $\text{cm}^{-1}$ , and the modes at 209 and 410  $\text{cm}^{-1}$  associated with the two Si neighbors of H. Except for the LVM at 2014  $\text{cm}^{-1}$ , all are pseudolocal modes [27] (pLVMs) which readily couple to bulk phonons. The energies of all the normal modes of the supercell are shown in Fig. 3. The modes whose energies peak sharply and repeatedly throughout the simulation are the 410  $\text{cm}^{-1}$  ( $B$ ) and 261  $\text{cm}^{-1}$  ( $C$  and  $D$ ) modes.

We performed four MD simulations, each at  $T = 50$ , 100, and 150 K. The decay process is always very much the same. The energy in the asymmetric stretch is absorbed by the 410 and 209  $\text{cm}^{-1}$  modes, which themselves decay almost immediately into bulk phonon modes. This is apparent when blowing up the inset in Fig. 3 (the inset contains  $\sim 12\,000$  time steps) to uncover the inner structure of the  $B$  and  $C$  peaks.

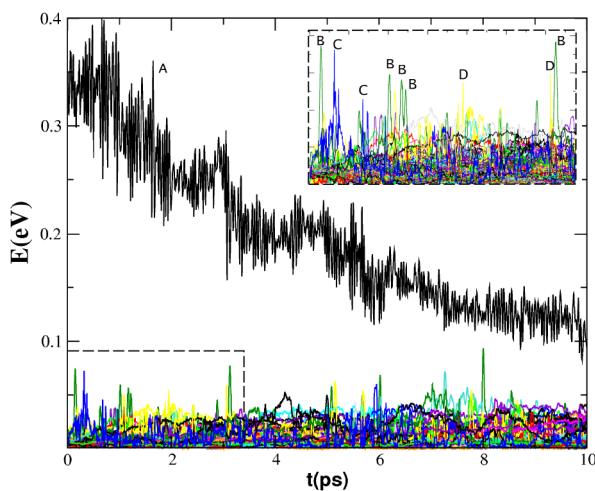


FIG. 3 (color online). Energies of all the normal modes in the supercell vs time during the decay of the 2014  $\text{cm}^{-1}$  mode of  $H_{BC}^+$  ( $A$ ) at  $T = 75$  K. The first 3.5 ps are enlarged in the inset (see text).

The details of the *fast* decay processes of  $H_{BC}^+$  and  $H_2^*$  are sensitive to the initial conditions. The random distributions of initial mode energies and phases affect the amplitude of a particular mode at  $t = 0$  and, if this mode happens to be a receiving mode, may cause different runs at the same temperature to produce somewhat different lifetimes. Therefore, for each temperature, we performed four runs for  $H_{BC}^+$  and six runs for  $H_2^*$  (experimentalists obtain an average of the  $\sim 10^{16}$   $\text{cm}^{-3}$  centers detected simultaneously). We averaged the energy of the excited mode over the various runs and fit the resulting curve to an exponential. The results, shown in Fig. 4, are in nice agreement with the measured temperature dependence of the lifetimes. Note that such an averaging is not necessary for very long lifetimes.

As  $T \rightarrow 0$ , the *classical* oscillation amplitudes vanish instead of approaching the zero-point amplitudes commensurate with the quantum mechanical ground state. In the real crystal, the amplitudes, anharmonic couplings, and, therefore, lifetimes become constant. In classical MD simulations, the amplitudes of the receiving modes and, therefore, the anharmonic couplings go to zero and the lifetimes become very long. We attempted to calculate the decay of  $H_{BC}^+$  at 0 K and indeed failed to observe a decay. The constant lifetimes observed below  $\sim 40$  K are zero-point oscillation effects which cannot be reproduced in our calculations.

The lifetime of the stretch mode of  $VH \cdot HV$  (295 ps at low temperatures [8,10]) is computationally challenging with a 0.3 fs time step. Figure 5 shows the energy of the two degenerate Si-H modes at 2092  $\text{cm}^{-1}$  for over 335 000 time steps at  $T = 200$  K. The decay is slow but steady. An exponential fit produces  $\tau \sim 170$  ps, reasonably close to the experimental value at this temperature  $\sim 200$  ps [8].  $VH \cdot HV$  has no pLVMs and its wag modes (597  $\text{cm}^{-1}$ ) do not couple to the 2092  $\text{cm}^{-1}$  mode. Plots of the time dependence of the energy of all the modes do not allow the identification of specific receiving modes, be-

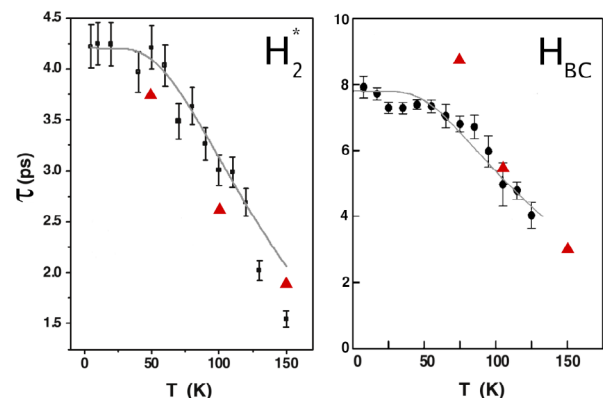


FIG. 4 (color online). The triangles (circles) show the calculated (measured [8]) lifetimes  $H_2^*$  and  $H_{BC}^+$ .

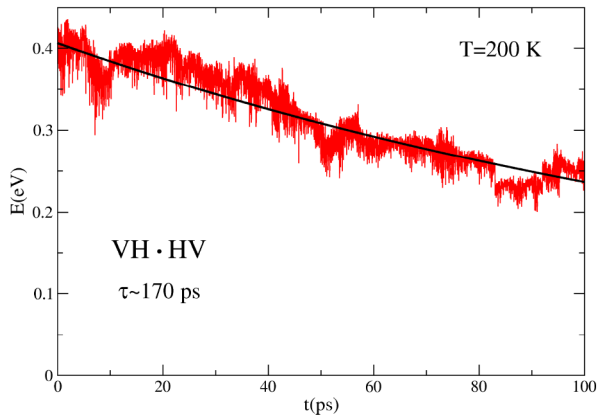


FIG. 5 (color online). Energy of the two degenerate Si-H stretch modes of  $VH \cdot HV$  vs time for about 335 000 time steps.

cause they have very short lifetimes and begin to decay into multiple bulk phonons as soon as their amplitude picks up.

Our calculations show that the decay of high-frequency LVMs depends on the existence of lower-lying LVMs as well as pLVMs in the vibrational spectra of the defect. In the case of  $H_2^*$ , the first step of the decay of the Si- $H_{BC}$  stretch ( $2126 \text{ cm}^{-1}$ ) is controlled by the Si- $H_{AB}$  stretch ( $1860 \text{ cm}^{-1}$ ) plus a pLVM at  $272 \text{ cm}^{-1}$  which involves oscillations of the two Si atoms bound to the Hs. In the case of the asymmetric stretch of  $H_{BC}^+$ , a defect that has no other LVMs, the decay is more complicated but clearly begins with pLVMs at 209 and  $410 \text{ cm}^{-1}$  (associated with the two Si neighbors of H), which themselves couple very efficiently to the wag modes of H and bulk phonons. Finally, the  $VH \cdot HV$  defect has no LVMs or pLVMs it can couple to. Coupling to the four wag modes, just above the  $\Gamma$  phonon, would involve a cumbersome “3.5”-phonon process. The decay of the stretch mode occurs by coupling to multiple bulk phonons, as discussed in the experimental work, and fits on the frequency-gap law. In conclusion, our first-principles calculations reproduce the experimental data above  $\sim 50 \text{ K}$  and demonstrate that the entire vibrational spectrum of a defect must be considered in order to understand the vibrational lifetime of high-frequency LVMs. This includes LVMs that are not IR active as well as pLVMs that are rarely measurable. Theory is required here.

This work is supported in part by a grant from the R. A. Welch Foundation and a contract from the National Renewable Energy Laboratory. Many thanks to Texas Tech’s High Performance Computer Center for generous amounts of CPU time.

\*Electronic address: stefan.estreicher@ttu.edu

[1] T.-C. Shen, C. Wang, G.C. Abeln, J.R. Tucker, J.W. Lyding, Ph. Avouris, and R.E. Walkup, *Science* **268**, 1590 (1995).

- [2] A. Stetsmans, *Phys. Rev. B* **61**, 8393 (2000); *J. Appl. Phys.* **88**, 489 (2000).
- [3] J.W. Lyding, K. Hess, and I.C. Kizilyalli, *Appl. Phys. Lett.* **68**, 2526 (1996).
- [4] L.C. Feldman, G. Lüpke, and N.H. Tolk, *Solid State Phenom.* **95–96**, 123 (2004).
- [5] R. Biswas, Y.-P.Li, and B.C. Pan, *Appl. Phys. Lett.* **72**, 3500 (1998); *J. Non-Cryst. Solids* **266–269**, 176 (2000).
- [6] M. Budde, G. Lüpke, C. Parks Cheney, N.H. Tolk, and L.C. Feldman, *Phys. Rev. Lett.* **85**, 1452 (2000).
- [7] G. Lüpke, N.H. Tolk, and L.C. Feldman, *J. Appl. Phys.* **93**, 1 (2003).
- [8] G. Lüpke, X. Zhang, B. Sun, A. Fraser, N.H. Tolk, and L.C. Feldman, *Phys. Rev. Lett.* **88**, 135501 (2002).
- [9] M. Budde, C. Parks Cheney, G. Lüpke, N.H. Tolk, and L.C. Feldman, *Phys. Rev. B* **63**, 195203 (2001).
- [10] M. Budde, G. Lüpke, E. Chen, X. Zhang, N.H. Tolk, L.C. Feldman, E. Tarhan, A.K. Ramdas, and M. Stavola, *Phys. Rev. Lett.* **87**, 145501 (2001).
- [11] A. Nitzan and J. Jortner, *Mol. Phys.* **25**, 713 (1973); A. Nitzan, S. Mukamel, and J. Jortner, *J. Chem. Phys.* **60**, 3929 (1974).
- [12] S.A. Egorov and J.L. Skinner, *J. Chem. Phys.* **103**, 1533 (1995).
- [13] B. Sun, G.A. Shi, S.V.S. Nageswara, M. Stavola, N.H. Tolk, S.K. Dixit, L.C. Feldman, and G. Lüpke, *Phys. Rev. Lett.* (to be published).
- [14] J. Fabianand and P.B. Allen, *Phys. Rev. Lett.* **77**, 3839 (1996).
- [15] S.R. Bickham and J.L. Feldman, *Phys. Rev. B* **57**, 12 234 (1998).
- [16] D. Sánchez-Portal, P. Ordejón, E. Artacho, and J.M. Soler, *Int. J. Quantum Chem.* **65**, 453 (1997).
- [17] E. Artacho, D. Sánchez-Portal, P. Ordejón, A. García, and J.M. Soler, *Phys. Status Solidi B* **215**, 809 (1999).
- [18] L. Kleiman and D.M. Bylander, *Phys. Rev. Lett.* **48**, 1425 (1982).
- [19] D.M. Ceperley and B.J. Adler, *Phys. Rev. Lett.* **45**, 566 (1980).
- [20] S. Perdew and A. Zunger, *Phys. Rev. B* **23**, 5048 (1981).
- [21] O.F. Sankey and D.J. Niklevski, *Phys. Rev. B* **40**, 3979 (1989); O.F. Sankey, D.J. Niklevski, D.A. Drabold, and J.D. Dow, *Phys. Rev. B* **41**, 12 750 (1990).
- [22] S. Baroni, P. Giannozzi, and A. Testa, *Phys. Rev. Lett.* **58**, 1861 (1987).
- [23] X. Gonze, *Phys. Rev. A* **52**, 1096 (1995); X. Gonze and C. Lee, *Phys. Rev. B* **55**, 10 355 (1997).
- [24] J.M. Pruneda, S.K. Estreicher, J. Junquera, J. Ferrer, and P. Ordejón, *Phys. Rev. B* **65**, 075210 (2002).
- [25] J.D. Holbeck, B. Bech Nielsen, R. Jones, P. Sitch, and S. Öberg, *Phys. Rev. Lett.* **71**, 875 (1993).
- [26] G. Peshlherbe, X. Wang, and W. Hase, in *Monte Carlo Methods in Chemical Physics*, edited by D.M. Ferguson, J. Ila Siepmann, and D.G. Truhlar (Wiley, New York, 1998).
- [27] S.K. Estreicher, D. West, J. Goss, S. Knack, and J. Weber, *Phys. Rev. Lett.* **90**, 035504 (2003); S.K. Estreicher, D. West, and M. Sanati, *Phys. Rev. B* **72**, 121201(R) (2005).